Fusion Engineering and Design 167 (2021) 112312

Contents lists available at ScienceDirect

Fusion Engineering and Design

journal homepage: www.elsevier.com/locate/fusengdes

Benchmark experiment for bismuth by slab samples with D-T neutron source

Y. Ding [a], Y. Nie [a,*], J. Ren [a], X. Ruan [a], Q. Zhao [a], Z. Hu [a,d], H. Wu [a], H. Zhang [a], K. Zhang [a], S. Zhang [b], D. Wang [b], R. Han [c]

[a] Key Laboratory of Nuclear Data, China Institute of Atomic Energy, Beijing, 102413, China
[b] College of Physics and Electronic Information, Inner Mongolia University for Nationalities, Tongliao, 028000, China
[c] Institute of Modern Physics, Chinese Academy of Sciences, Lanzhou, 730000, China
[d] School of Nuclear Science and Technology, Lanzhou University, Lanzhou, 730000, China

ARTICLE INFO

Keywords:
Benchmark experiment
D-T neutron source
Neutron leakage spectrum
TOF technique
C/E value

ABSTRACT

A benchmark experiment is carried out with slab sample to validate nuclear data of bismuth by measurement of leakage neutron spectra from 0.8–16 MeV. The measured experiments are performed at China Institute of Atomic Energy with the integral benchmark facility established on the D–T neutron generator. The neutrons leaking from the sample are recorded at the measuring angle of 60° and 120° by time-of-flight technique. To make understanding of the impact of accuracy of data files in evaluated library on the neutron transport simulation, the calculation is carried out by MCNP-4C code with a series of latest available evaluated libraries. The calculated spectra are analyzed by comparing with experimental ones in neutron spectrum shape and C/E values. The result indicates that the theoretical simulation with different data libraries overestimated or underestimated the measured ones in some energy ranges, and the secondary neutron energy distribution and angular distribution in data files have been present to explain it.

1. Introduction

Lead-bismuth eutectic (LBE) has become the most promising candidate for Generation IV nuclear system and accelerator-driven sub-critical system (ADS) as cooling material, due to its obvious advantages in neutronics and safe operation [1]. Moreover, as an ideal spallation target in ADS, LBE can achieve high neutron yield with good thermal physical properties, and can realize good coupling with the reactor [2, 3].

Lead (Pb) and Bismuth (Bi) are the essential component of LBE, and simulation of neutron transport in these materials have a considerable impact on the design parameters. However, Pb and Bi have not yet received the same attention as common structural materials or the major actinide elements in nuclear data field, and the careful evaluation has not been regarded as crucial part for existing nuclear data libraries [4]. Some organizations have carried out benchmark experiments for Pb in recent years [5–11], but few for Bi. S.P. Simakov et al. [12] first carried out the benchmark test of Bi in 1992, measuring the leakage spectrum from a 9 cm thick Bi shell sample with T(d, n) source, and measurement with ^{252}Cf spontaneous-fission neutron source was carried out after modifying the experimental layout [13]. These experiments can only provide limited data for modifying the evaluated nuclear data of Bi. So, it is necessary to carry out new integral experiments to validate the current evaluated libraries for the design of new nuclear applications and reactors. China Institute of Atomic Energy (CIAE) has established an integral benchmark facility, and a series of benchmark tests have been successfully done on it [14–19]. In this work, an integral experiment for Bi at 60° and 120° is performed by measuring leakage neutrons from 0.8−16 MeV with time-of-flight (TOF) technique, while the Monte Carlo simulation is performed by MCNP-4C code [20], in which the Bi data are taken from JENDL-4.0 [21]、CENDL-3.2 [22]、JEFF-3.3 [23] and ENDF/B-VIII.0 [24] evaluated libraries respectively. The benchmark results are analyzed by the comparison between experiment and simulation in the spectrum shape and the C/E values of leakage neutron in specified energy ranges.

* Corresponding author.
E-mail address: nieyb@163.com (Y. Nie).

https://doi.org/10.1016/j.fusengdes.2021.112312
Received 23 September 2020; Received in revised form 26 January 2021; Accepted 1 February 2021
Available online 3 March 2021

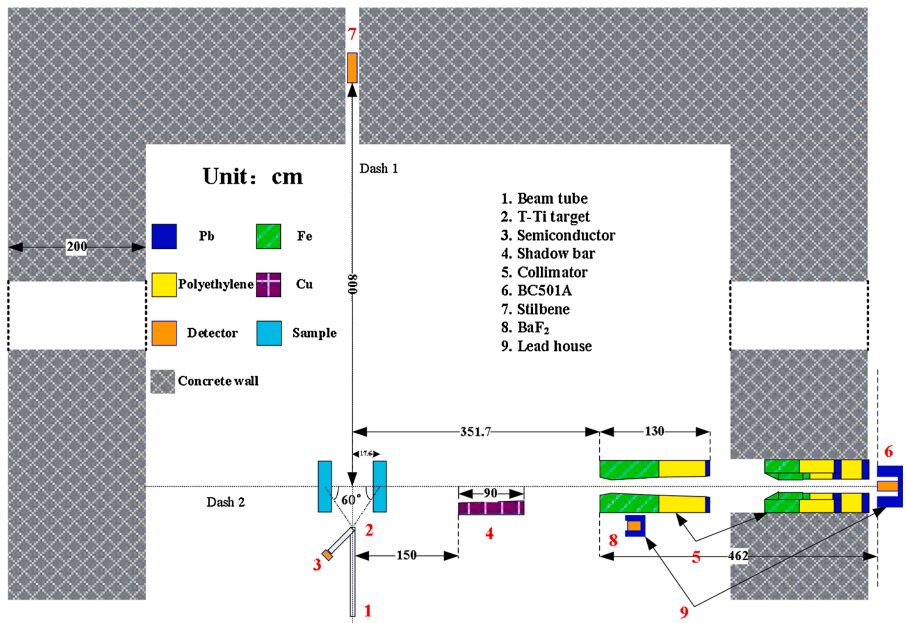

Fig. 1. Experimental arrangement for measuring the neutron leakage spectra from bismuth slabs. (Dash 1: the incident deuteron (D^+) beam line; Dash 2: the leakage neutron direction).

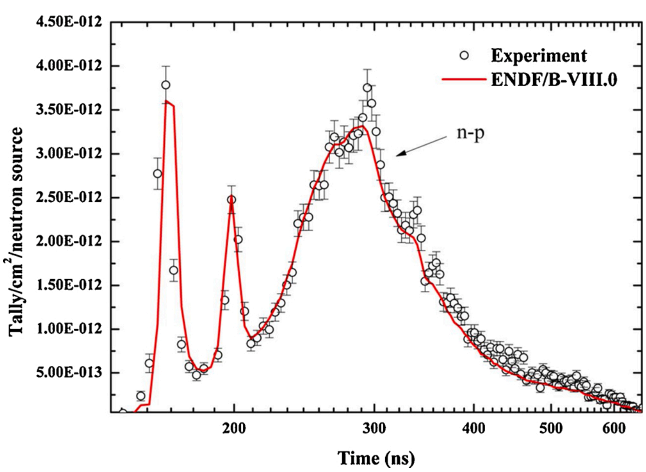

Fig. 2. The measured leakage neutron TOF spectrum with a polyethylene sample (30 cm × 30 cm × 6 cm) at 60°.

2. Experiment

Fig. 1 shows the layout of the integral benchmark facility at CIAE. This section describes the experiment briefly since the details introduced elsewhere [25,26].

The surface area of sample is 30 cm × 30 cm, and the thicknesses are 5 cm, 10 cm and 15 cm, corresponding to 0.76, 1.52 and 2.28 mean free paths for 14.5 MeV neutrons, respectively. The sample has high purity Bi of 99.9%, and 9.700 g/cm^3 in density. The neutrons are generated by D^+ beam bombarding a Tritium–Titanium (T-Ti) target, and the neutron yield is determined by counting the associated ^{4}He particles with an Au-Si surface barrier semiconductor. Three detectors are applied in the measurement: the TOF spectra of source neutron are recorded by a stilbene scintillation crystal, while the associated gamma rays from the target are recorded by a BaF_2 scintillation crystal, the leakage neutron spectra from sample are detected by a BC501A liquid scintillation detector. The first two detectors are combined to obtain the time structure of the pulsed beam. The leakage neutrons are measured at two scattering angles about 60° and 120°. As shown in Fig. 1, the sample is put at the right side of the Dash 1 when measuring angle is 60°with the flight distance about 796.4 cm. Once moving the sample along the Dash 2 (leakage neutron direction) to left side of the Dash 1, the measuring angle is changed to be 120°, and the flight distance is about 831.6 cm.

The elastic scattering of neutron and hydrogen (n–p scattering) is considered as the standard cross section, therefore, benchmark experiment with polyethylene is carried out to ensure the reliability of the system. The result of polyethylene (30 cm × 30 cm× 6 cm) experiment is in agreement with the calculated one by ENDF/B-VIII.0 library as shown in Fig. 2. The comparison between experimental result and calculated one of n–p scattering peak indicates that the experimental system is reliable, meanwhile we can obtain a coefficient $B^1 = 1.5 \times 10^6$ with Eq. (1),

$$N_n = \frac{N_p^e}{N_p^c} = B^1 \times N_\alpha^p \tag{1}$$

where N_n is the number of neutrons from T (d, n) ^{4}He reaction for polyethylene, N_P^e is the number of n–p scattering neutrons detected from polyethylene, N_P^c is the number of n–p scattering neutrons calculated by MCNP code from polyethylene (per source neutron), and N_α^p is the number of alpha particles detected for polyethylene.

In this experiment, the uncertainties include the statistical and the systematic uncertainties. Due to the measured data is normalized by n–p scattering of polyethylene sample with Eq. (2),

$$\frac{N_B^e}{N_n} = \frac{N_B^e}{B^1 \times N_\alpha^B} = \frac{N_B^e \times N_P^c \times N_\alpha^P}{N_P^e \times N_\alpha^B} \tag{2}$$

where N_B^e is the number of neutrons detected from bismuth per time bin and N_α^B is the number of alpha particles detected for bismuth. Most of the systematic uncertainties are suppressed which described in detail in the previous work [17]. The systematic uncertainty is mainly caused by the relative neutron detection efficiency (3%) and the scattering angle ambiguity (2%). The statistical uncertainty is about 5%, which includes N_B^e (~5%), N_P^c (< 0.5%), N_α^P (< 0.5%), N_P^e (< 0.5%) and N_α^B (< 0.5%).

Table 1
Nuclear data libraries used in this work.

Evaluated library name	Nuclear data quoted	
	Bi	Other materials
CENDL-3.2	CENDL-3.2	ENDF/B-VIII.0
ENDF/B-VIII.0	ENDF/B-VIII.0	ENDF/B-VIII.0
JENDL-4.0	JENDL-4.0	ENDF/B-VIII.0
JEFF-3.3	JEFF-3.3	ENDF/B-VIII.0

3. Monte Carlo simulation

The experimental results are analyzed by comparing with MCNP-4C calculating results. For validation of evaluated data, four evaluated data libraries are selected as listed in Table 1.

In the MCNP simulation, the experimental apparatus as well as the shielding and collimating system are modeled precisely in Fig. 3. The measured time structure of source neutron spectrum and theoretically calculated energy and angular distribution by the TARGET code [27] are used to describe the neutron source condition. The leakage neutrons are recorded by point detector. The uncertainty of the simulation is less than 1% for each time bin when the neutron histories are set to 10^9.

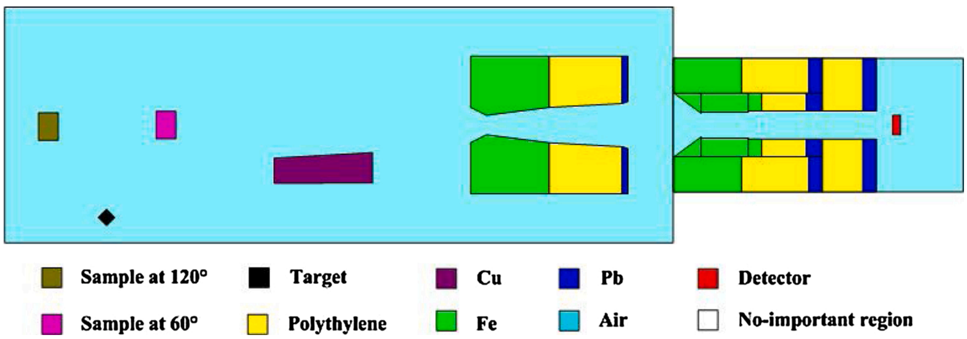

Fig. 3. Model for the MCNP simulation.

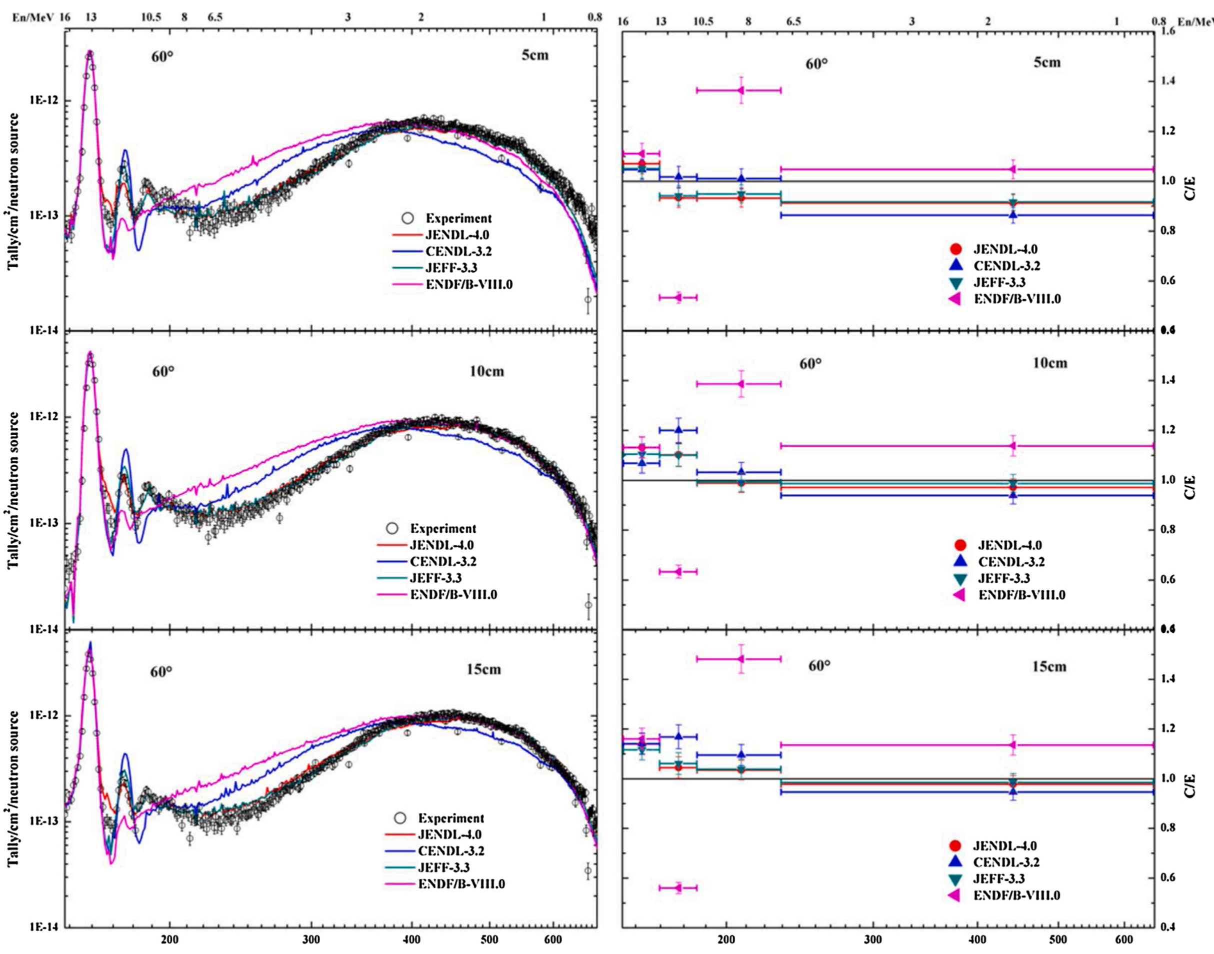

Fig. 4. The comparison of measured and calculated leakage neutron spectra from bismuth sample and the C/E values integrated over the specified energy ranges at 60°.

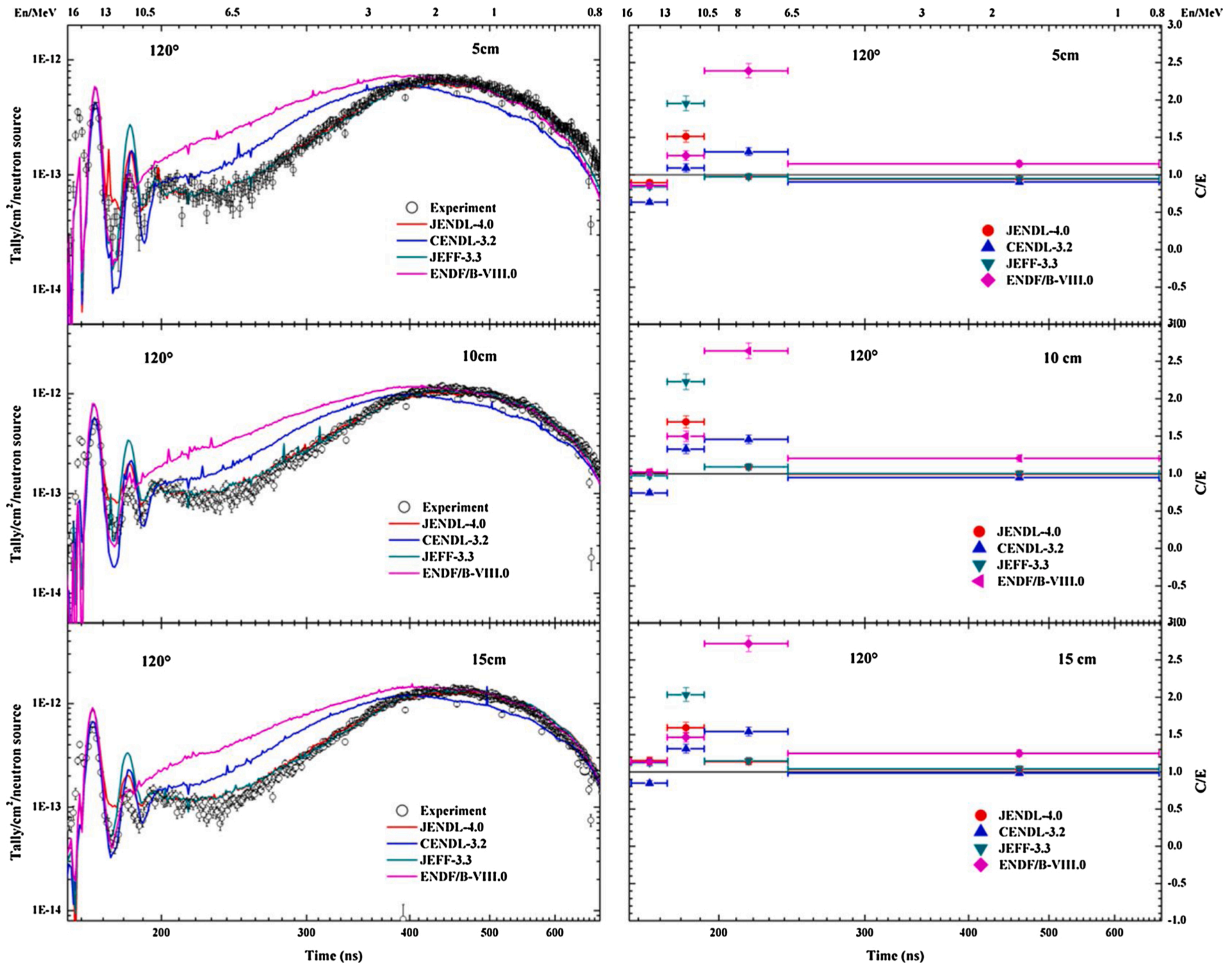

Fig. 5. The comparison of measured and calculated leakage neutron spectra from bismuth sample and the C/E values integrated over the specified energy ranges at 120°.

4. Results and discussion

The experimental measured leakage spectra are compared with theoretical simulated ones and a series of C/E values of partial spectra integrated over five ranges are obtained. Fig. 4 displays the leakage spectra from the sample of different thickness at 60° with corresponding C/E values in different energy range, and Fig. 5 is for 120°. It can be seen that the calculated spectra with ENDF/B-VIII.0 and CENDL-3.2 show a large overestimation from 2 to 10.5 MeV. In addition, the C/E values are listed in Table 2.

Comparing with experimental spectra, there are discrepancies existing in certain energy range among four libraries calculated results. In order to further analyze the results and determine which partial cross section in the evaluated data files should be reinvestigated. We retrieved the total and partial cross section from the data files and plotted in Fig. 6. It has been found that the (n, np)、(n, 3n) and (n, nα) cross section affect the total spectrum in minor contributions. Therefore, we believe that the (n, el), (n, inl), and (n, 2n) reactions should be taken into consideration. Dividing the benchmark test results into four main energy ranges, the following conclusions can be obtained:

(1) In 13−16 MeV, the elastic scattering channel makes most contribution. At 60°, the calculated spectra with four different data files are discrepant from the measured ones within 15%. At 120°, calculations with CENDL-3.2 library fairly underestimate the experimental results by more than 35%, while the remaining three libraries show better agreement with experiment.
(2) In 10.5−13 MeV, the discrete inelastic scattering ((n, n')d) channel contribute most. The calculation with ENDF/B-VIII.0 library shows larger difference from the experimental spectrum with a underestimation about 35–50% at 60°, while those with the JENDL-4.0 and JEFF-3.3 give better agreement with the experiment with difference about 10%. At 120°, the calculated results with four libraries are higher than experiment, especially the JEFF-3.3 library whose calculated results are around 1.2 times the experimental results.
(3) In 6.5−10.5 MeV, the secondary neutron originates from the continuous inelastic scattering ((n, n')c) channel most. The ENDF/B-VIII.0 gives a large overestimation at both 60°and 120°, especially at 120°, the C/E value even reaches about 1.7. As for the results obtained from JENDL-4.0 and JEFF-3.3 are similar to each other and give justifiable predictions, while CENDL-3.2 calculations predict the experiment well at 60°but give larger difference about 30–50% at 120°.
(4) In 0.8–6.5 MeV, the (n, 2n) reaction contributes most. The calculated results with ENDF/B-VIII.0 library are discrepant from the measured ones more than 15% at 120°, while those with others data files predict the experiment well with a underestimation less than 10%.

The discrepancies may be caused by the angular distribution of elastic scattering and the secondary neutron energy distribution (SED) in evaluated database. As depicted in Fig. 7, the angular distribution of the elastic scattering implies that the spectrum with CENDL-3.2 becomes

Table 2
The comparisons of C/E values between the calculated and measured spectra integrated over specified energy ranges and total energy ranges.

Time (ns)	Energy (MeV)	C/E (JENDL-4.0)	C/E (CENDL-3.2)	C/E (JEFF-3.3)	C/E (ENDF/B-VIII.0)
60°(30 cm × 30 cm×5 cm)					
150−166	13–16	1.070 ± 0.040	1.047 ± 0.039	1.051 ± 0.039	1.110 ± 0.041
166−184	10.5−13	0.934 ± 0.039	1.017 ± 0.042	0.942 ± 0.039	0.534 ± 0.022
184−232	6.5−10.5	0.932 ± 0.036	1.011 ± 0.039	0.949 ± 0.037	1.364 ± 0.053
232−414	2.0−6.5	0.931 ± 0.034	1.133 ± 0.041	0.929 ± 0.034	1.353 ± 0.049
414−650	0.8−2.0	0.900 ± 0.033	0.673 ± 0.024	0.909 ± 0.033	0.835 ± 0.030
150−650	0.8−16	0.925 ± 0.033	0.882 ± 0.032	0.927 ± 0.033	1.055 ± 0.038
60°(30 cm × 30 cm×10 cm)					
150−166	13−16	1.131 ± 0.042	1.068 ± 0.039	1.105 ± 0.041	1.132 ± 0.042
166−184	10.5−13	1.102 ± 0.045	1.200 ± 0.049	1.100 ± 0.045	0.634 ± 0.026
184−232	6.5−10.5	0.989 ± 0.038	1.032 ± 0.039	0.992 ± 0.038	1.386 ± 0.053
232−414	2.0−6.5	0.969 ± 0.035	1.220 ± 0.044	0.969 ± 0.035	1.431 ± 0.052
414−650	0.8−2.0	0.972 ± 0.035	0.767 ± 0.028	0.998 ± 0.036	0.958 ± 0.035
150−650	0.8−16	0.984 ± 0.036	0.954 ± 0.034	0.997 ± 0.036	1.139 ± 0.041
60°(30 cm × 30 cm×15 cm)					
150−166	13−16	1.140 ± 0.042	1.141 ± 0.042	1.116 ± 0.041	1.160 ± 0.043
166−184	10.5−13	1.045 ± 0.043	1.168 ± 0.048	1.061 ± 0.044	0.560 ± 0.023
184−232	6.5−10.5	1.034 ± 0.040	1.095 ± 0.042	1.038 ± 0.040	1.482 ± 0.057
232−414	2.0−6.5	0.977 ± 0.035	1.234 ± 0.045	0.959 ± 0.035	1.419 ± 0.051
414−650	0.8−2.0	0.978 ± 0.035	0.789 ± 0.029	0.999 ± 0.036	0.979 ± 0.035
150−650	0.8−16	0.991 ± 0.0356	0.966 ± 0.035	0.996 ± 0.036	1.140 ± 0.041
120°(30 cm × 30 cm×5 cm)					
156−173	13−16	0.895 ± 0.036	0.634 ± 0.026	0.840 ± 0.034	0.857 ± 0.035
173−192	10.5−13	1.513 ± 0.076	1.090 ± 0.055	1.955 ± 0.099	1.256 ± 0.063
192−242	6.5−10.5	0.975 ± 0.039	1.308 ± 0.053	0.975 ± 0.039	2.391 ± 0.096
242−432	2.0−6.5	0.950 ± 0.034	1.195 ± 0.043	0.948 ± 0.034	1.523 ± 0.055
432−678	0.8−2.0	0.937 ± 0.034	0.707 ± 0.026	0.947 ± 0.034	0.895 ± 0.032
156−678	0.8−16	0.945 ± 0.034	0.908 ± 0.033	0.952 ± 0.034	1.169 ± 0.042
120°(30 cm × 30 cm×10 cm)					
156−173	13−16	1.017 ± 0.040	0.741 ± 0.029	0.972 ± 0.039	1.020 ± 0.041
173−192	10.5−13	1.690 ± 0.080	1.328 ± 0.063	2.227 ± 0.105	1.498 ± 0.071
192−242	6.5−10.5	1.088 ± 0.043	1.456 ± 0.057	1.090 ± 0.043	2.638 ± 0.103
242−432	2.0−6.5	0.987 ± 0.036	1.236 ± 0.045	0.989 ± 0.036	1.566 ± 0.057
432−678	0.8−2.0	0.995 ± 0.036	0.767 ± 0.028	1.009 ± 0.036	0.980 ± 0.035
156−678	0.8−16	0.997 ± 0.036	0.953 ± 0.034	1.008 ± 0.036	1.226 ± 0.044
120°(30 cm × 30 cm×15 cm)					
156−173	13−16	1.151 ± 0.045	0.846 ± 0.033	1.122 ± 0.044	1.132 ± 0.045
173−192	10.5−13	1.592 ± 0.072	1.310 ± 0.059	2.035 ± 0.092	1.462 ± 0.066
192−242	6.5−10.5	1.138 ± 0.044	1.539 ± 0.060	1.147 ± 0.045	2.719 ± 0.106
242−432	2.0−6.5	0.992 ± 0.036	1.238 ± 0.045	0.988 ± 0.036	1.557 ± 0.056
432−678	0.8−2.0	1.055 ± 0.038	0.826 ± 0.030	1.074 ± 0.039	1.058 ± 0.038
156−678	0.8−16	1.037 ± 0.037	0.992 ± 0.036	1.049 ± 0.038	1.271 ± 0.046

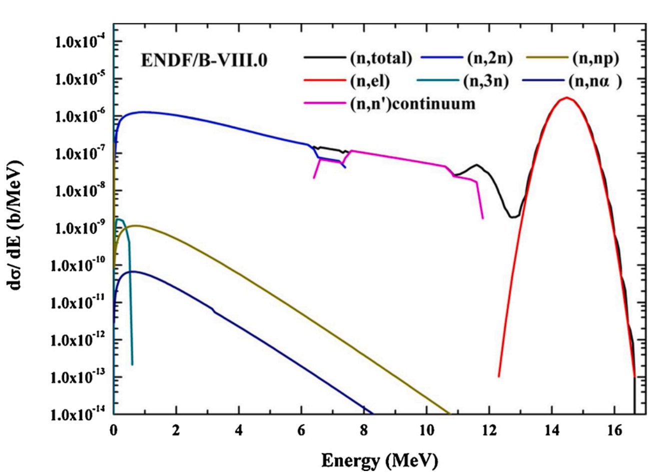

Fig. 6. The distributions of leakage neutron spectra from different reactions for bismuth.
(Retrieved from the ENDF/B-VIII.0 library).

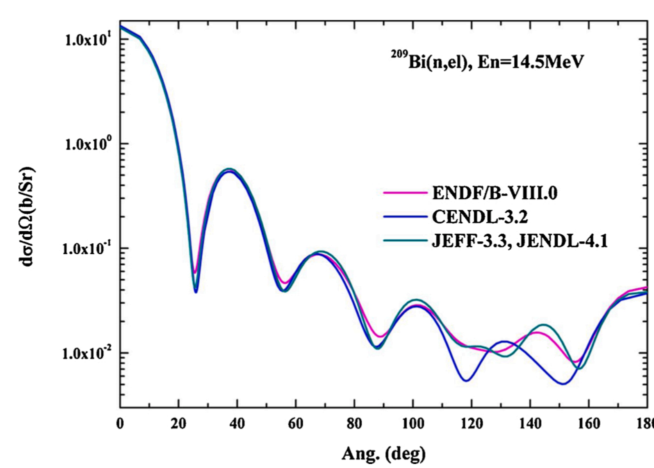

Fig. 7. The angular distributions of elastic cross section for bismuth from different evaluated files.

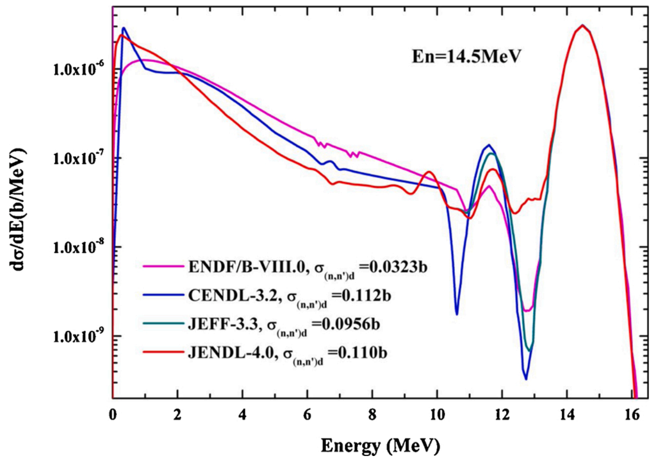

Fig. 8. The energy distributions of emission neutrons for bismuth at incident neutron energy of 14.5 MeV.

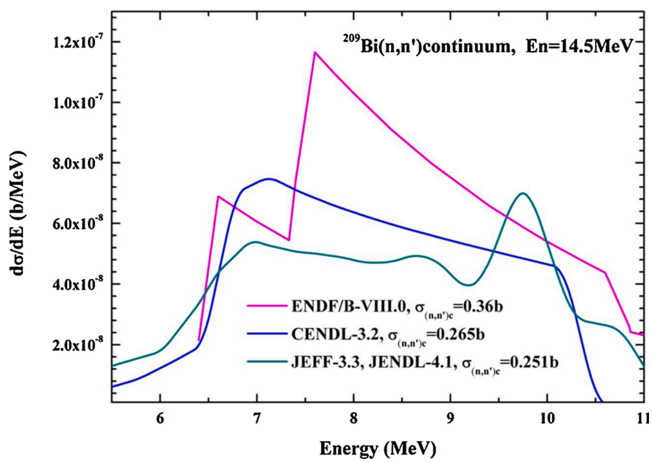

Fig. 9. The contributions from the continuum inelastic scattering for bismuth at the incident neutron energy of 14.5 MeV.

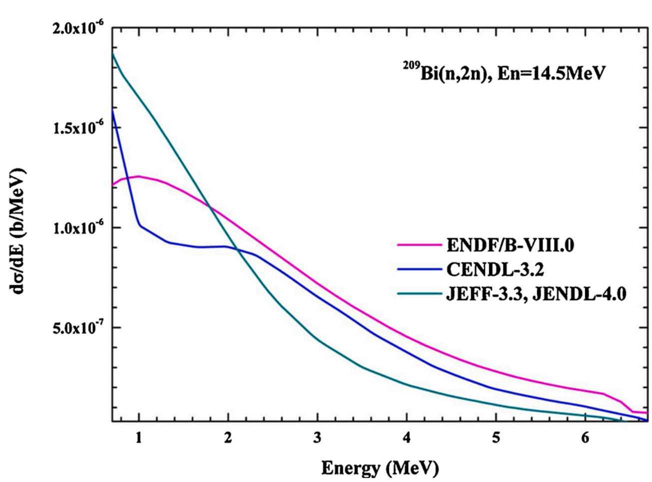

Fig. 10. The neutron spectra from (n, 2n) reactions at the incident neutron energy of 14.5 MeV.

lower at 120°, which might be the main cause for the underestimate of CENDL-3.2 in this energy range.

The SED of total reaction channels extracted from different evaluated data files are plotted in Fig. 8, the partial spectra of ENDF/B-VIII.0 in 8.5−13 MeV is lower than the others libraries. Meanwhile, the cross section of (n, n')d ($\sigma_{(n,\ n')d}$) is 0.0323b which also lower than those from the others libraries. The cross section of ((n, n')d) from the ENDF/B-VIII.0 data file may need a reevaluation.

Fig. 9 shows the SED of (n, n')c for ^{209}Bi which extracted from four evaluated data files, the cross section of (n, n')c is 0.36b in ENDF/B-VIII.0 which gives a general overestimation, and the simulated spectrum with ENDF/B-VIII.0 get richer becoming a "peak" at the 7.5−9 MeV energy range. All above may be the main cause for the discrepancies between the calculation and experiment for ENDF/B-VIII.0 in this energy range.

The SED of (n, 2n) for ^{209}Bi from four libraries are plotted in Fig. 10. The calculated spectrum with ENDF/B-VIII.0 is lower than those from JEFF-3.3 and JENDL-4.0 at 0.8−2 MeV low energy range, while is higher at the 2–6.5 MeV.

5. Summary

The measurement of leakage neutron spectrum in the energy range from 0.8 MeV to 16 MeV is conducted to validate the available Bi data in existing evaluated libraries. Several latest available libraries including JENDL-4.0, CENDL-3.2, JEFF-3.3 and ENDF/B-VIII.0 are taken into account. The calculations are performed by MCNP-4C code and compared with measured ones. The experimental results can be well reproduced by the calculations in high energy range (13−16 MeV), but some discrepancies exist in inelastic scattering energy range. The calculation with ENDF/B-VIII.0 gives a general underestimation with experiment in 10.5−13 MeV at 60° and a certain amount of overestimation in 6.5−10.5 MeV at both 60° and 120° are observed. The calculated results with JENDL-4.0 and JEFF-3.3 libraries give satisfactory agreement with the measured ones from 0.8 MeV to 10.5 MeV. We believe that improper evaluation of the angular distribution and the secondary neutron energy distribution has led to the discrepancies between calculation and experiment. Overall, this benchmark experiment provides valuable data for validation of nuclear data of Bi, and lays a foundation for the subsequent adjustments to the CENDL-3.2 in the further work.

Declaration of Competing Interest

The authors report no declarations of interest.

Acknowledgments

This work is supported by the National Natural Science Foundation of China under Grant Number 11775311. The authors gratefully acknowledge H. Chen's team for their excellent operation of the D-T neutron source in this experiment.

References

[1] W.U. Yi-can, et al., Development status and prospects of Lead-based reactors, Nucl. Sci. Eng. 35 (2015) 213–221.
[2] S.S. Kapoor, Accelerator-driven sub-critical reactor system (ADS) for nuclear energy generation, Editorial 59 (2002) 941–950.
[3] P.A. Gokhale, et al., Accelerator driven systems (ADS) for energy production and waste transmutation: international trends in R&D, Prog. Nucl. Energy 48 (2006) 91–102.
[4] A.J. Koning, et al., New nuclear data libraries for lead and bismuth and their impact on accelerator-driven systems design, Nucl. Sci. Eng. 156 (2007) 357–390.
[5] T. Elfruth, et al., The neutron multiplication of lead at 14 MeV neutron incidence energy, Atomkernenergie-Kerntechnik 49 (1987) 121–125.
[6] S.P. Simakov, et al., 14 MeV Facility and Research in IPPE, Report INDC(CCP)-351, IAEA, 1993.
[7] A.A. Androsenko, et al., Measurements and comparison with calculations of neutron leakage spectra from U, Pb, Be spheres with central 14MeV neutron source, Kernenergie 10 (1988) 422.
[8] Y. Oyama, et al., Experimental Results of Angular Neutron Flux Spectra Leaking From Slabs of Fusion Reactor Candidate Materials (I), JAERI-M90-092, 1990.
[9] H. Maekawa, et al., Experiment on angular neutron flux spectra from lead slabs bombarded by D-T neutrons, Fusion Eng. Des. 18 (1991) 287.

[10] S. Kwon, et al., Lead benchmark experiment with DT neutrons at JAEA/FNS, Fusion Sci. Technol. 72 (2017) 362–367.
[11] K. Ochiai, et al., D-t neutronics benchmark experiment on lead at JAEA/FNS, J. Korean Phys. Soc. 59 (2011) 1953–1956.
[12] S.P. Simakov, et al., Neutron leakage spectra from Be, Al, Fe, Ni, Pb, LiPb, Bi, U and Th sphere with T(d,n) and ^{252}Cf neutron source, Fusion Technol. 1993 (1992) 1489–1493.
[13] S.P. Simakov, et al., Benchmarking of evaluated nuclear data for bismuth by spherical shell transmission experiments with central T(d,n) and Cf-252 neutron sources, Fusion Eng. Des. 46 (89) (1999).
[14] Y. Nie, et al., Benchmarking of evaluated nuclear data for uranium by a 14.8 MeV neutron leakage spectra experiment with slab sample, Ann. Nucl. Energy 37 (2010) 1456–1460.
[15] R. Han, Et. al., Fast neutron scattering on Gallium target at 14.8 MeV, Nucl. Phy. A 936 (2015) 17–28.
[16] S. Zhang, Z. Chen, et al., Measurement of leakage neutron spectra for Tungsten with D-T neutrons and validation of evaluated nuclear data, Fusion Eng. Des. 92 (2015) 41–45.
[17] Y. Nie, et al., The benchmark experiment on slab beryllium with D–T neutrons for validation of evaluated nuclear data, Fusion Eng. Des. 105 (2016) 8–14.
[18] Z. Lin, et al., Benchmarking of 232Th evaluation by a 14.8 MeV neutron leakage spectra experiment with slab samples, Ann. Nucl. Energy 96 (2016) 181–186.
[19] Q. Sun, et al., Experiment on uranium slabs of different thicknesses with D-T neutrons and T validation of evaluated nuclear data, Fusion Eng. Des. 125 (2017) 9–17.
[20] B.J.F, MCNPTM -A General Monte Carlo N-Particle Transport Code, Version 4C., 2000.
[21] K. Shibata, et al., JENDL-4.0: a new library for nuclear science and engineering, J. Nucl. Sci. Technol. 48 (2011) 1–30.
[22] Z.G. Ge, et al., CENDL-3.2: the new version of chinese general purpose evaluated nuclear data library, EPJ Web conf. 239 (2020), 09001.
[23] O. Cabellos, et al., Benchmarking and validation activities within JEFF project, EPJ Web Conf. 146 (2017), 06004. Article.
[24] D.A. Brown, et al., ENDF/B-VIII.0: the 8th major release of the nuclear reaction data library with CIELO-project cross sections, new standards and thermal scattering data, Nucl. Data Sheets 148 (2018) 1–142.
[25] Y. Ding, et al., The benchmark experiment on slab iron with D-T neutrons for validation of evaluated nuclear data, Ann. Nucl. Energy 132 (2019) 236–242.
[26] Y. Nie, et al., Benchmark experiments with slab sample using time-of-flight technique at CIAE, Ann. Nucl. Energy 136 (2020).
[27] D. Schlegel, TARGET User's Manual, Laborbericht PTB-6.42-05-2, Braunschweig, Germany, 2005.